 CMES, vol.67, no.1, pp.55-77, 2010

A Novel Meshless Method for Solving the Second Kind of Fredholm Integral Equations

Hua Zou[1] **and Hua Li**[1,2]

Abstract: A novel meshless technique termed the Random Integral Quadrature (RIQ) method is developed in this paper for solving the generalized integral equations. By the RIQ method, the governing equations in the integral form are discretized directly with the field nodes distributed randomly or uniformly, which is achieved by discretizing the integral governing equations with the generalized integral quadrature (GIQ) technique over a set of background virtual nodes, and then interpolating the function values at the virtual nodes over a set of field nodes with Local Kriging method, where the field nodes are distributed either randomly or uniformly. The RIQ method is a meshless technique since it doesn't require any approximation cells, but a set of field nodes distributed either randomly or uniformly in the computational domain. In order to validate the RIQ method, the second kind of Fredholm integral equations in one-, two- and three-dimensional domains are solved via both randomly and uniformly distributed field nodes. Corresponding convergence rate is also studied for each of the case studies. The numerical solutions of all these case studies demonstrate that the RIQ method can achieve highly computational accuracy, even if only a few field nodes are scattered in the domains, and also make good convergence rates.

Keywords: Meshless method, Generalized integral quadrature method, Kriging interpolation function, Random integral quadrature method, Fredholm integral equation

1 Introduction

Integral equations have applications in engineering and sciences, such as heat and mass transfer, oscillation theory, elasticity and plasticity, fluid dynamics, electrostatics and electrodynamics, medicine and biomechanics, game theory, economics,

[1] School of Mechanical and Aerospace Engineering, Nanyang Technological University, 50 Nanyang Avenue, Singapore 639798, Republic of Singapore

[2] Corresponding author, Tel.: + 65 6790 4953; Fax: + 65 6792 4062; Email address: lihua@ntu.edu.sg (Hua Li)

etc. According to the types of the integral domain, the integral equations can be classified into two categories, Fredholm integral equation and Volterra integral equation. In this paper, the second kind of Fredholm integral equation is discussed only. So far great attention has been attracted to the techniques for the solution of the second kind of Fredholm integral equations, for example, the conventional successive approximations method, the successive substitutions method, the Adomian decomposition method [Rahman (2007)] and other numerical methods [Babolian, Abbasbandy and Fattahzadeh (2008); Farnoosh and Ebrahimi (2008); Maleknejad and Karami (2005)].

Recently the meshless method has achieved great progress, in order to overcome the drawbacks of the traditional mesh-based methods, such as the finite element method (FEM). In general, there are two types of meshless methods, the strong-form and weak-form methods. The strong-form meshless methods include the finite point method [Oñate, Idelsohn, Zienkiewicz and Taylor (1996)], Hermite cloud method [Li, Ng, Cheng and Lam (2003)], the gradient smoothing method [Liu, Zhang, Lam, Li, Xu, Zhong and Han (2008)] and so on. The weak-form meshless methods include the smooth particle hydrodynamics method [Lucy (1977)], the diffuse element method [Nayroles, Touzot and Villon (1992)], the element-free Galerkin method [Belytschko, Lu and Gu (1994)], the reproducing kernel particle method [Liu, Sukky and Yi Fei (1995)], the meshless local Petrov-Galerkin method [Atluri and Zhu (1998)] and the local Kriging method [Li, Wang and Lam (2004)].

However, the meshless methods mentioned above are mainly used to solve partial differential equations although there are also several meshless methods which can solve integral equations directly, such as the generalized integral quadrature (GIQ) method [Shu, Khoo, Chew and Yeo (1996)]. The GIQ technique always requires regular domains in which the field nodes are scattered along straight lines for solving the integral equations. This constrains the applications of the GIQ method.

In this paper, a novel meshless method, termed the random integral quadrature (RIQ) method, is proposed for solving the second kind of Fredholm integral equations. It combines the GIQ technique with the Kriging interpolation function together, where the GIQ technique is used first to discretize the integral governing equation over the virtual nodes along straight lines in the domain. Then the Kriging interpolation function is used to approximate the field function values at the virtual nodes through the field nodes scattered uniformly or randomly. Because the Kriging interpolation function is employed here, the field nodes can be distributed either randomly or uniformly. Several case studies in one-, two- and three- dimensional domains for numerical validation are presented to examine the RIQ method as well as to study the convergence rates. The numerical results reveal that the present RIQ method is accurate and efficient enough for numerically solving the

second kind of Fredholm integral equations.

2 Kriging interpolation

The Kriging interpolation technique is a generalized linear regression used to formulate an optimal estimator in a sense of the minimum mean square error, which was introduced by Krige for moving averages to avoid systematic errors in interpolation [Krige (1951)]. This technique possesses several advantages. The first is that it compensates for the effects of data clustering, assigning individual points within a cluster less weight than isolated data points. The second is that it provides the estimation error along with estimate of the variable itself. The third is that the availability of estimation error provides the basis for stochastic simulation of possible realizations of estimator. So far the Kriging technique has become a fundamental tool in the geostrategic and other fields. Due to the rigorous theoretical basis, the Kriging method can ensure theoretical accuracy of interpolation. In addition, the shape functions constructed have the delta properties, due to the present interpolation passing node. Thus the boundary conditions can be imposed easily. Moreover, the computing algorithm of the Kriging function is quite simple, such that it is a good interpolation function.

Let's have a computational domain Ω discretized by a number of nodes $\mathbf{x}_i$ $(1 \leq i \leq N)$, where N is the number of total nodes in the domain. As per Kriging interpolation [Li, Wang and Lam (2004)], the approximation of a function $u(\mathbf{x})$ is given by

$$u^h(\mathbf{x}) = \sum_{i=1}^{N} \lambda_i u(\mathbf{x}_i) \tag{1}$$

where $u^h(\mathbf{x})$ is the approximation of the function value $u(\mathbf{x})$ at the node $\mathbf{x}$, $u(\mathbf{x}_i)$ the function value at the corresponding field node $\mathbf{x}_i$. λ_i is the weighting coefficient related to the field nodes $\mathbf{x}_i$ and is determined by minimizing the squared variance of the estimation error $E\left\{\left[u(\mathbf{x}) - u^h(\mathbf{x})\right]^2\right\}$.

If there is no bias in the estimation formula given by Eq. (1), the expected values of $u(\mathbf{x})$ and $u^h(\mathbf{x})$ have to be equal,

$$E\left[u(\mathbf{x})\right] = E\left[u^h(\mathbf{x})\right] = \sum_{i=1}^{N} \lambda_i E\left[u(\mathbf{x}_i)\right] \tag{2}$$

The random field function $u(\mathbf{x})$ is decomposed into two parts as,

$$u(\mathbf{x}) = R(\mathbf{x}) + m(\mathbf{x}) \tag{3}$$

where the first part $R(\mathbf{x})$ has a stationary mean of 0 and a stationary covariance with a function of lag h as,

$$E[R(\mathbf{x})] = 0 \tag{4}$$

$$\mathrm{Cov}[R(\mathbf{x}), R(\mathbf{x}+\mathbf{h})] = E[R(\mathbf{x}) \cdot R(\mathbf{x}+\mathbf{h})] \tag{5}$$

The second part $m(\mathbf{x}) = E[u(\mathbf{x})]$ is called the drift. The expected value of $u(\mathbf{x})$ is described as

$$m(\mathbf{x}) = \sum_{i=1}^{N} \lambda_i m(\mathbf{x}_i) \tag{6}$$

It is assumed here that the drift belongs to the linear subspace S and is taken as a linear polynomial. Eq. (6) thus becomes

$$p_k(\mathbf{x}) = \sum_{i=1}^{N} \lambda_i p_k(\mathbf{x}_i), \quad 1 \le k \le l \tag{7}$$

where p is the basis in S. In one-dimensional space, the linear basis is given by

$$\mathbf{p}^{\mathrm{T}}(\mathbf{x}) = [1 \quad x], \quad l = 2 \tag{8}$$

In two-dimensional space, it is written as

$$\mathbf{p}^{\mathrm{T}}(\mathbf{x}) = [1 \quad x \quad y], \quad l = 3 \tag{9}$$

The squared variance of the estimation error can be computed by

$$E\left\{\left[u(\mathbf{x}) - \sum_{i=1}^{N} \lambda_i u(\mathbf{x}_i)\right]^2\right\} = E[u(\mathbf{x})]^2 - 2\sum_{i=1}^{N} \lambda_i E[u(\mathbf{x}) u(\mathbf{x}_i)] + \sum_{i=1}^{N}\sum_{j=1}^{N} \lambda_i \lambda_j E[u(\mathbf{x}_i) u(\mathbf{x}_j)] \tag{10}$$

By minimizing Eq. (10) with respect to the coefficients λ_i under l linear constraints that satisfy the no bias conditions, the solution is characterized by a linear system of $(N+l)$ equations related to unknowns $\lambda_1, \lambda_2, \cdots, \lambda_N$ and $\mu_1, \mu_2, \cdots, \mu_l$,

$$\begin{aligned} &\sum_{j=1}^{N} \lambda_j E[u(\mathbf{x}_i) u(\mathbf{x}_j)] + \sum_{k=1}^{l} \mu_k p_k(\mathbf{x}_i) = E[u(\mathbf{x}) u(\mathbf{x}_i)] \\ &\sum_{j=1}^{N} \lambda_j p_k(\mathbf{x}_j) = p_k(\mathbf{x}) \end{aligned} \tag{11}$$

where coefficients μ_k are the Lagrange multipliers associated with the constraints. The covariance $E[u(\mathbf{x})u(\mathbf{x}_i)]$ is replaced with the semivariogram $\gamma(h)$, where h is the Euclidean distance between $\mathbf{x}$ and $\mathbf{x}_i$, and the Gaussian semivariogram model is employed as

$$\gamma(h) = c_0\left(1 - e^{-3\left(\frac{\|h\|}{a_0}\right)^2}\right) \tag{12}$$

where c_0 is the sill representing the average variance of points at such a distance away from the point considered that there is no influence between the points. a_0 is the range representing the distance, at which there is no longer a correlation between the points and it is taken as

$$a_0 = \alpha \cdot \beta \cdot d_{\min} \tag{13}$$

where α is a coefficient, β a scaling parameter, and $d_{\min}$ the shortest distance between an interpolation point and its neighboring points.

As such, the Kriging system (11) is written in the matrix form as

$$\mathbf{AY} = \mathbf{b} \tag{14}$$

where

$$\mathbf{A} = \begin{bmatrix} \mathbf{R} & \mathbf{P} \\ \mathbf{P}^T & 0 \end{bmatrix} = \begin{bmatrix} \gamma(\mathrm{x}_1,\mathrm{x}_1) & \cdots & \gamma(\mathrm{x}_1,\mathrm{x}_N) & p_1(\mathrm{x}_1) & \cdots & p_l(\mathrm{x}_1) \\ \vdots & \ddots & \vdots & \vdots & \ddots & \vdots \\ \gamma(\mathbf{x}_N,\mathbf{x}_1) & \cdots & \gamma(\mathbf{x}_N,\mathbf{x}_N) & p_1(\mathbf{x}_N) & \cdots & p_l(\mathbf{x}_N) \\ p_1(\mathbf{x}_1) & \cdots & p_1(\mathbf{x}_N) & 0 & \cdots & 0 \\ \vdots & \ddots & \vdots & \vdots & \ddots & \vdots \\ p_l(\mathbf{x}_1) & \cdots & p_l(\mathbf{x}_N) & 0 & \cdots & 0 \end{bmatrix} \tag{15}$$

$$\mathbf{Y} = \begin{bmatrix} \lambda_1 & \lambda_2 & \cdots & \lambda_N & \mu_1 & \mu_2 & \cdots & \mu_N \end{bmatrix}^T \tag{16}$$

$$\mathbf{b} = [\gamma(\mathbf{x}) \quad \mathbf{p}(\mathbf{x})] = \begin{bmatrix} \gamma(\mathbf{x},\mathbf{x}_1) & \cdots & \gamma(\mathbf{x},\mathbf{x}_N) & p_1(\mathbf{x}) & \cdots & p_l(\mathbf{x}) \end{bmatrix}^T \tag{17}$$

One can obtain λ_i by solving this system of linear equations, Substituting λ_i into Eq. (1), the estimating value is obtained as

$$u^h(\mathbf{x}) = \varphi(\mathbf{x})u \tag{18}$$

where $\mathbf{u} = \begin{bmatrix} \mathbf{u}(\mathbf{x}_1) & \mathbf{u}(\mathbf{x}_2) & \cdots & \mathbf{u}(\mathbf{x}_N) \end{bmatrix}^T$, $\varphi(\mathbf{x})$ is the shape function matrix and is calculated by

$$\varphi(\mathbf{x}) = \gamma^T\mathbf{S} + \mathbf{p}^T\mathbf{Q}; \quad \mathbf{S} = \mathbf{R}^{-1}(\mathbf{I} - \mathbf{PQ}); \quad \mathbf{Q} = \left(\mathbf{P^T R^{-1} P}\right)^{-1}\mathbf{P}^T\mathbf{R}^{-1} \tag{19}$$

3 Generalized integral quadrature technique

The generalized integral quadrature (GIQ) technique follows the similar concept to the polynomial-based partial differential quadrature (PDQ) .[Shu (2000)]. If the whole integral domain Ω is decomposed into n sub-domains, the integral term over the sub-domain Ω_i is discretized as follows .[Shu (2000)],

$$\int_{\Omega_i} u(\mathbf{x})\, d\mathbf{x} = \sum_{k=1}^{M} \mathbf{w}_{ik} u\left(\mathbf{x}^k\right) \tag{20}$$

where $i = 1, 2, \cdots n$, M is the total number of scattered nodes in the whole domain Ω, $\mathbf{w}_{ik}$ the weighting coefficient related to the node $\mathbf{x}^k$. After the integral term over each sub-domain is determined, we can sum them together and thus the integral over the whole domain is given by

$$\int_{\Omega} u(\mathbf{x})\, d\mathbf{x} = \int_{\Omega_1} u(\mathbf{x})\, d\mathbf{x} + \int_{\Omega_2} u(\mathbf{x})\, d\mathbf{x} + \cdots + \int_{\Omega_n} u(\mathbf{x})\, d\mathbf{x} = \sum_{i=1}^{n} \sum_{k=1}^{M} \mathbf{w}_{ik} u\left(\mathbf{x}^k\right) \tag{21}$$

The key of this approach is to obtain the weighting coefficients, but it is not easy to be determined in the integral quadrature. However, this can easily be achieved by the first-order derivative in polynomial-based differential quadraqure (PDQ) .[Shu (2000)]. By the PDQ approach, a function is approximated by a high-order polynomial or the Fourier series if the function is smooth in the entire domain of a problem. Usually a polynomial-based approximation is adopted for simplification with high accuracy. The high-order polynomial involves all the functional values in the whole domain. As such, the integration of the function over the sub-domain can be calculated by integrating the approximated polynomial. Let's take the one-dimensional case as an example to illustrate the computation of the weighting coefficients.

Consider a function $\varphi(x)$ to be sufficiently continuous over the domain $[a, b]$ with M scatted nodes in the domain. The function is approximated by an $(M-1)$ th order polynomial. In particular, when the functional values are known at the M grid points, $\varphi(x)$ can be approximated by the Lagrange interpolation polynomials which are related to the node values at all the virtual nodes. As a result, the integral of this approximated polynomial over a sub-domain $[x_i, x_j]$ may involve the function values over the whole domain. The integral of $\varphi(x)$ over a sub-domain is given as

$$\int_{x_i}^{x_j} \varphi(x) dx = \sum_{k=1}^{M} w_k^{ij} \varphi(x_k) \tag{22}$$

where x_i and x_j are the coordinates of the bound of the integral, and they can be altered according to the situation. w_k^{ij} is the weighting coefficient, where $k =$

1, 2, ..., M. If the Lagrange interpolation polynomials $r_k(x)$ are chosen as the basis polynomials, w_k^{ij} is determined by

$$w_k^{ij} = \int_{x_i}^{x_j} r_k(x)dx \tag{23}$$

It is difficult to calculate w_k^{ij} directly from Eq. (23). However, w_k^{ij} could be determined by the weighting coefficients of the first-order derivative by PDQ approach .[Shu (2000)].

Let's define

$$\varphi(x) = \frac{du(x)}{dx} \tag{24}$$

where it is noted that, $u(x)$ is an Mth order polynomial if $\varphi(x)$ is an $(M-1)$ th order polynomial. Here is approximated by

$$\varphi(x) = a_0 + a_1 x + \cdots + a_{M-1}x^{M-1} \tag{25}$$

where a_0, a_1, $\cdots$, a_{M-1} are constants. Integrating Eq. (25) from a constant c to x in both sides gives

$$u(x) = \int_c^x \varphi(t)\,dt + u(c) = \psi(x,c) + u(c) \tag{26}$$

where

$$\psi(x,c) = x\left(a_0 + \frac{a_1}{2}x + \cdots + \frac{a_{M-1}}{M}x^{M-1}\right) - c\left(a_0 + \frac{a_1}{2}c + \cdots + \frac{a_{M-1}}{M}c^{M-1}\right) \tag{27}$$

It is known that $\psi(x,c)$ constitutes a M dimensional linear polynomial vector space. Let's choose a set of basis polynomials as

$$p_k(x) = (x-c)\,r_k(x) \tag{28}$$

where $r_k(x)$ is the Lagrange interpolation polynomial. By the PDQ approach [Shu, Khoo and Yeo (1994)], one can have

$$\psi_x(x_i,c) = \sum_{j=1}^{M} a_{ij}\psi(x_j,c) \text{ for } i = 1, 2, \cdots, M \tag{29}$$

where a_{ij} are the weighting coefficients. Using the same method as in the PDQ approach, and substituting Eq. (28) into Eq. (29), and one can have

$$a_{ii} = b_{ii} + \frac{1}{x_i - c}; \quad a_{ij} = \frac{x_i - c}{x_j - c}b_{ij} \text{ if } j \neq i \tag{30}$$

where b_{ij} are the weighting coefficients of the first-order derivative in PDQ approach, and expressed as .[Shu (2000)]

$$b_{ij} = \frac{1}{x_j - x_i} \prod_{k=1,k\neq i,j}^{M} \left(\frac{x_i - x_k}{x_j - x_k} \right); \quad b_{ii} = - \sum_{j=1,j\neq i}^{M} b_{ij}^{(1)} \tag{31}$$

Thus, the weighting coefficients in Eq. (29) are obtained by

$$\begin{aligned} a_{ij} &= \frac{x_i - c}{x_j - c} \times \frac{1}{x_j - x_i} \prod_{k=1,k\neq i,j}^{M} \left(\frac{x_i - x_k}{x_j - x_k} \right) \\ a_{ii} &= - \sum_{j=1,j\neq i}^{M} w_{ij}^{(1)} + \frac{1}{x_i - c} \end{aligned} \tag{32}$$

By the above equations, it is no way to choose c as the coordinates of the virtual nodes x_i. Here Eq. (29) can be written in the matrix form of

$$[\psi_x] = [A]\,[\psi] \tag{33}$$

where

$$\begin{aligned} [\psi] &= [\psi(x_1, c), \psi(x_2, c), \cdots \psi(x_M, c)]^T \\ [\psi_x] &= [\varphi] = [\psi_x(x_1, c), \psi_x(x_2, c), \cdots \psi_x(x_M, c)]^T \end{aligned} \tag{34}$$

Substituting Eqs. (24) and (26) into Eq. (33) gives

$$[\varphi] = [A]\,[\psi] \tag{35}$$

By setting $[W] = [A]^{-1}$, Eq. (35) is rewritten as

$$\int_c^{x_i} \varphi(x)dx = \sum_{k=1}^{M} w_{ik}\varphi(x_k), \quad for\ i = 1,\ 2,\ \cdots,\ M \tag{36}$$

As a result,

$$\int_{x_i}^{x_j} \varphi(x)dx = \sum_{k=1}^{M} \left(w_{jk} - w_{ik} \right) \varphi(x_k) \tag{37}$$

The weighting coefficients of the GIQ technique are thus given as follows,

$$w_k^{ij} = w_{jk} - w_{ik} \tag{38}$$

The same approach can be extended to multi-dimensional cases. For example, a two-dimensional case is considered here. Let the whole computational domain be $a \le x \le b$, $c \le y \le d$, which is decomposed with MX virtual nodes in the x direction, and MY virtual nodes in the y direction. Let $\varphi(x,y)$ be continuous in the entire domain and consider an integral of $\varphi(x,y)$ over a sub-domain. By the same approach as the above one-dimensional case, the formulation of the two-dimensional integral of over the sub-domain $x_i \le x \le x_j$ and $y_l \le y \le y_m$ is given as

$$\int_{x_i}^{x_j}\int_{y_l}^{y_m} \varphi(x,y)\,dxdy = \sum_{n=1}^{MX}\sum_{k=1}^{MY} (w_{jn}-w_{in})(w_{mk}-w_{lk})\varphi(x_n,y_k) \tag{39}$$

where w_{jn} and w_{mk} are the weighting coefficients of the one-dimensional integral in the $x-$ and $y-$ directions, respectively, and are given by

$$\begin{aligned} w_{jn}-w_{in} &= \int_{x_i}^{x_j} r_n(x)dx \quad i,j,n = 1,2,\cdots,MX \\ w_{mk}-w_{lk} &= \int_{y_l}^{y_m} s_k(y)dy \quad l,m,k = 1,2,\cdots,MY \end{aligned} \tag{40}$$

where $r_n(x)$ and $s_k(y)$ are the Lagrange interpolation polynomials in the $x-$ and $y-$directions respectively. Similar to the one-dimensional case, and can be determined by the PDQ approach.

For the three-dimensional case, let the function $\varphi(x,y,z)$ be continuous in the domain , , $g \le z \le h$, which is discretized with MX virtual nodes in the $x-$direction, MY virtual nodes in the $y-$ direction and MZ virtual nodes in the $z-$ direction. The integral of over the sub-domain , , and $z_e \le z \le z_q$ can be approximated as

$$\begin{aligned} &\int_{x_i}^{x_j}\int_{y_l}^{y_m}\int_{z_e}^{z_q} \varphi(x,y)\,dxdy = \\ &\qquad \sum_{n=1}^{MX}\sum_{k=1}^{MY}\sum_{p=1}^{MZ} (w_{jn}-w_{in})(w_{mk}-w_{lk})(w_{qp}-w_{ep})\varphi(x_n,y_k,z_p) \end{aligned} \tag{41}$$

where w_{qp} is the weighting coefficient of the one-dimensional integral in the z direction, and is given by

$$w_{qp}-w_{ep} = \int_{z_e}^{z_q} t_p(z)\,dz \quad e,\ p,\ q = 1,\ 2,\ \cdots,\ MZ \tag{42}$$

where $t_p(z)$ is the Lagrange interpolation polynomial in the z direction.

4 Random integral quadrature

The motivation of developing the random integral quadrature (RIQ) method is to extend the application of the generalized integral quadrature (GIQ) technique. As well known, the GIQ technique always requires regular domains, in which the field nodes are always required to lie along a straight line. This becomes one of drawbacks of the GIQ technique and constrains its application. In order to overcome the drawback, the present RIQ method is proposed in this paper. It is achieved by discretizing the integral governing equations with the GIQ technique over a set of background virtual nodes, and then interpolating the function values of the virtual nodes over a set of field nodes with the Local Kriging method. By using the interpolation function, the field nodes can be distributed either randomly or uniformly.

For formulation of the RIQ method, let's consider the second kind of Fredholm integral equation as example,

$$u(\mathbf{x}) = g(\mathbf{x}) + \lambda \int_{\Omega} k(\mathbf{x},\mathbf{t})\, u(\mathbf{t})\, d\Omega \tag{43}$$

where $g(\mathbf{x})$ is a known function, $k(\mathbf{x},\mathbf{t})$ the kernel function, λ a constant, Ω the bounded computational domain, and $u(\mathbf{x})$ the unknown function.

4.1 Two sets of nodes

The present RIQ method requires two sets of nodes, namely the virtual nodes and the field nodes. The virtual nodes $\mathbf{x}^j\,(1 \le j \le M)$ are scattered along straight lines so as to implement the GIQ technique, where M is the number of the virtual nodes scattered in the computational domain. It is noted that the virtual nodes can be scattered along straight lines in various manners, for example, uniformly or cosine distribution. In this paper, the cosine distribution is employed for the virtual nodes. In one-dimensional case, if the computational domain is defined as $a \le x \le b$, the virtual nodes are distributed as

$$x^j = a + \left(\frac{1 - \cos\left(\frac{j-1}{M-1}\pi\right)}{2} \right) \times L \tag{44}$$

where $L = b - a$. In multi-dimensional case, the coordinates of the virtual nodes are determined along the number of nodes in each direction. The field nodes $\mathbf{x}_i$ (i =1,2,...N, and N is the number of field nodes) are scattered either randomly or uniformly and they are used for interpolation by the Kriging interpolation function.

4.2 Discretize the governing equation

After the virtual nodes are scattered in the computational domain, the integral governing equation is discretized over the virtual node $\mathbf{x}^j$ as

$$u^h\left(\mathbf{x}^j\right) = g\left(\mathbf{x}^j\right) + \lambda \sum_{k=1}^{M} w_{jk} K\left(\mathbf{x}^j, \mathbf{t}^k\right) u^h\left(\mathbf{t}^k\right) \tag{45}$$

where $\mathbf{x}^j$ and $\mathbf{t}^k$ are the virtual nodes, w_{jk} is the GIQ weighting coefficient for the jth virtual node, $u^h\left(\mathbf{x}^j\right)$ is the approximation of the function value over the virtual node $\mathbf{x}^j$. In order to use the Kriging interpolation as a matter of convenience, Eq. (45) is written in a matrix form of

$$\mathbf{QU} = \mathbf{G} \tag{46}$$

where $\mathbf{Q}$ is the final coefficient matrix as

$$\mathbf{Q} = \mathbf{I} - \lambda \times \begin{bmatrix} w_{11}K\left(\mathbf{x}^1, \mathbf{t}^1\right) & w_{12}K\left(\mathbf{x}^1, \mathbf{t}^2\right) & \cdots & w_{1M}K\left(\mathbf{x}^1, \mathbf{t}^M\right) \\ w_{21}K\left(\mathbf{x}^2, \mathbf{t}^1\right) & \cdots & \ddots & \vdots \\ \vdots & \vdots & \ddots & w_{(M-1)M}K\left(\mathbf{x}^{M-1}, \mathbf{t}^M\right) \\ w_{M1}K\left(\mathbf{x}^M, \mathbf{t}^1\right) & \cdots & w_{M(M-1)}K\left(\mathbf{x}^M, \mathbf{t}^{M-1}\right) & w_{MM}K\left(\mathbf{x}^M, \mathbf{t}^M\right) \end{bmatrix} \tag{47}$$

$\mathbf{U}$ is the vector of approximate function values over all the virtual nodes,

$$\mathbf{U} = \begin{bmatrix} u^h\left(\mathbf{x}^1\right) & u^h\left(\mathbf{x}^2\right) & \cdots & u^h\left(\mathbf{x}^M\right) \end{bmatrix}^{\mathbf{T}} \tag{48}$$

$\mathbf{G}$ is the right hand side vector, and can be easily filled by substituting the coordinate values of the virtual nodes,

$$\mathbf{G} = \begin{bmatrix} g\left(\mathbf{x}^1\right) & g\left(\mathbf{x}^2\right) & \cdots & g\left(\mathbf{x}^M\right) \end{bmatrix}^{\mathbf{T}} \tag{49}$$

4.3 Interpolation of virtual nodes

After the integral governing equation is discretized by the GIQ technique, a system of algebraic equations is obtained. The approximation function values over each of the virtual nodes are then interpolated by the Kriging technique over the field nodes in the whole domain,

$$u^h\left(\mathbf{x}^j\right) = \sum_{i=1}^{N} \varphi_j\left(\mathbf{x}_i\right) u\left(\mathbf{x}_i\right) \tag{50}$$

where $u^h\left(x^j\right)$ is the approximation of the function value at the virtual node x^j. $\varphi_j\left(x_i\right)$ is the shape function at the ith field node, and $u\left(x_i\right)$ is the function value at the ith field nodes. The shape function matrix is constructed by Eq. (19), and thus Eq. (50) is written in the matrix form

$$\begin{bmatrix} u^h\left(\mathbf{x}^1\right) \\ u^h\left(\mathbf{x}^2\right) \\ \vdots \\ u^h\left(\mathbf{x}^M\right) \end{bmatrix} = \begin{bmatrix} \varphi_1\left(\mathbf{x}_1\right) & \varphi_1\left(\mathbf{x}_2\right) & \cdots & \varphi_1\left(\mathbf{x}_N\right) \\ \varphi_2\left(\mathbf{x}_1\right) & \cdots & \ddots & \vdots \\ \vdots & \vdots & \ddots & \varphi_{M-1}\left(\mathbf{x}_N\right) \\ \varphi_M\left(\mathbf{x}_1\right) & \cdots & \varphi_M\left(\mathbf{x}_{N-1}\right) & \varphi_M\left(\mathbf{x}_N\right) \end{bmatrix} \begin{bmatrix} u\left(\mathbf{x}_1\right) \\ u\left(\mathbf{x}_2\right) \\ \vdots \\ u\left(\mathbf{x}_N\right) \end{bmatrix} \tag{51}$$

or simplified by

$$\mathbf{U} = \Phi \mathbf{U}' \tag{52}$$

4.4 Finalization of discrete system

The system of the algebraic equations is finally obtained by substituting Eq. (52) into Eq. (46), and is written as

$$\mathbf{C}\mathbf{U}^{'} = \mathbf{G} \tag{53}$$

It is noted that the size of the matrix $\mathbf{Q}$ is $M \times M$, and that of the shape function matrix is $M \times N$. As a result, the size of the final coefficients matrix $\mathbf{C}$ is $M \times N$, and $\mathbf{U}^{'} = \left[u\left(\mathbf{x}_1\right), u\left(\mathbf{x}_2\right), \cdots u\left(\mathbf{x}_N\right)\right]^{\mathbf{T}}$.

4.5 Implementation of the algebraic system

As mentioned above, the integral governing equation is discretized firstly over the virtual nodes, and then interpolated by the Kriging interpolation function, which leads to an over-determined system of equations $\mathbf{C}\mathbf{U}^{'} = \mathbf{G}$. Here the number of equations corresponds to the virtual nodes, while the number of the unknown function values corresponds to the field nodes. In order to obtain the unique and accurate solution of this system therefore, it is suggested that the number of the virtual nodes is more than the number of the field nodes. Then the least square approximation is employed to solve the final system, by which the rectangular matrix $\mathbf{C}$ is converted to a square matrix by multiplying $\mathbf{C}^T$ in both sides of the equation $\mathbf{C}\mathbf{U}^{'} = \mathbf{G}$. As such, the residual error $\mathbf{R} = \mathbf{C}\mathbf{U} - \mathbf{G}$ is minimized. Finally the approximate function values of the over-determined system are obtained. The solution of this algebraic system is the approximate function values over the field nodes due to the delta property of the Kriging interpolation method.

5 Numerical experiment and convergence study

Several one-, two- and three-dimensional cases of the second kind of Fredholm integral equations are studied here to demonstrate the performance of the RIQ method. The convergence rate is also examined for each case, by using a global error ε defined as [Mukherjee and Mukherjee (1997)],

$$\varepsilon = \frac{1}{|u|_{\max}} \sqrt{\frac{1}{N} \sum_{i=1}^{N} \left(u_i - u_i^h\right)^2} \tag{54}$$

where ε is defined as the global error for the numerical solution, N is the number of the total field nodes. u_i and u_i^h are the analytical exact and the numerical solutions at the i^{th} field node, respectively. $|u|_{\max}$ is the maximum absolute value of the analytical exact solution.

As well known, the second kind of Fredholm integral equation is generally clarified as

$$\varphi(\mathbf{x}) = f(\mathbf{x}) + \lambda \int_D K(\mathbf{x},\mathbf{y})\, \varphi(\mathbf{y})\, d\mathbf{y} \tag{55}$$

where $\lambda \neq 0$ is a parameter, and D a closed bound set in real space and independent of the filed variable. $K(\mathbf{x},\mathbf{y})$ is the integrable kernel function, and $f(\mathbf{x})$ a known function.

5.1 One-dimensional Fredholm integral equation

The first case study for one-dimensional Fredholm integral equation is given as

$$y(t) = e^{2t+\frac{1}{3}} - \frac{1}{3} \int_0^1 \left(e^{2t-\frac{5}{3}s}\right) y(s)\, ds \tag{56}$$

The exact solution of this problem is $y(t) = e^{2t}$ [Babolian, Marzban and Salmani (2008)]. In this case, both the kernel and the known functions are the exponential function as well as the exact solution. This problem is solved via the field nodes distributed uniformly and randomly with the cosine distributed virtual nodes. Totally 90 virtual nodes are used with 3, 5, 10, 20, 40, 60 field nodes respectively. As the first study, the linear basis is employed as the polynomial basis of the shape function and Fig. 1 is plotted to show the convergence rate of this problem using the RIQ method, where the global error is calculated by Eq. (54), and h is the nodal spacing for the field nodes distributed uniformly or the average nodal spacing for the field nodes distributed randomly, for comparison of the results via the field nodes distributed uniformly and randomly. It is observed from Fig. 1 that the

global errors for both the field nodes distributed uniformly and randomly are almost at the same level. Actually when the number of field nodes is equal to 3, the global errors for the field nodes distributed uniformly and randomly are 1.2674E-2 and 1.5500E-2 respectively, while the values of global errors are equal to 1.9140E-5 and 2.4774E-5 respectively for the field nodes distributed uniformly and randomly when the number of field nodes is 60. The convergence rates are 1.7434 and 1.8083 respectively for the field nodes distributed uniformly and randomly. In this example, the global error for the field nodes distributed uniformly seems to be slightly smaller than that for the field nodes distributed randomly, while the convergence rate for the field nodes distributed randomly is slightly higher than that for the field nodes distributed uniformly. It is thus conclude that the RIQ method can handle well the field nodes distributed uniformly and randomly.

The same problem is also solved again by the quadratic basis that is used as the polynomial basis of the shape function, and the convergence curves are plotted in Fig. 2. It is found from this figure that, when the nodal spacing is large, the global errors for the field nodes distributed randomly are larger than those for the field nodes distributed uniformly. However, as the nodal spacing decreases, the difference of the global errors between both the sets of field nodes becomes smaller and smaller. In other words, the numerical results always converge to the exact solution as the nodal spacing reduces, whether the field nodes scattered in the computational domain are random or uniform. The global errors are 1.2600E-2 and 1.9200E-2 respectively for 3 field nodes distributed uniformly and randomly, while they become 1.9859E-5 and 2.1672E-5 for the 60 field nodes respectively. The convergence rates are equal to 2.4136 and 1.7794 respectively for the field nodes distributed uniformly and randomly.

Fig. 3 is plotted to show the variation of the global errors with the number of the field nodes, for comparison of the numerical results obtained via the linear basis and the quadratic basis respectively, where the numerical results via the linear basis and the quadratic basis are obtained by the same set of field nodes. Obviously they are almost equal to each other when the field nodes are scattered uniformly. However, for the field nodes distributed randomly, the numerical results by the linear basis are better than those by the quadratic basis if fewer field nodes are used, but finally they all converge to the exact solution.

The second case study for more complex one-dimensional Fredholm integral equation is given as follows,

$$\varphi(x) = f(x) + \int_0^1 e^{x+s}\varphi(s)\,ds \tag{57}$$

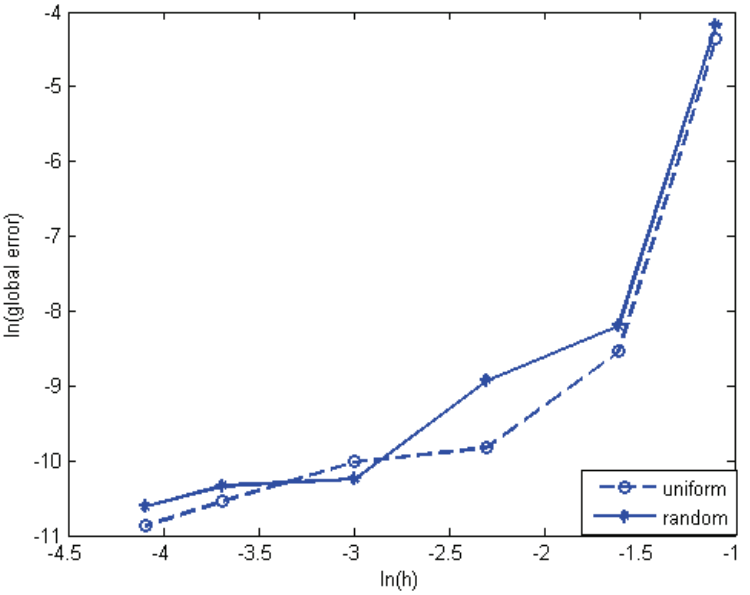

Figure 1: Convergence rates for the first case study of 1-D Fredholm integral equation via the field nodes distributed randomly and uniformly using the linear basis.

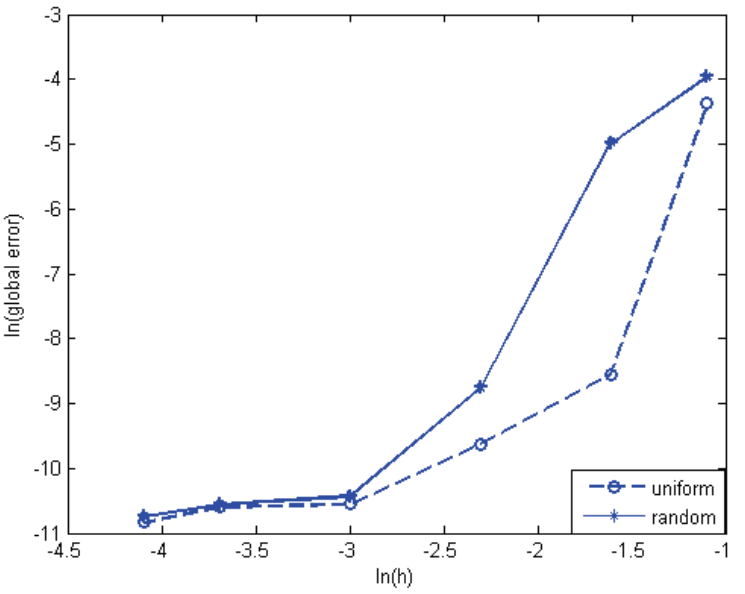

Figure 2: Convergence rates for the first case study of the 1-D Fredholm integral equation via field nodes distributed randomly and uniformly using quadratic basis.

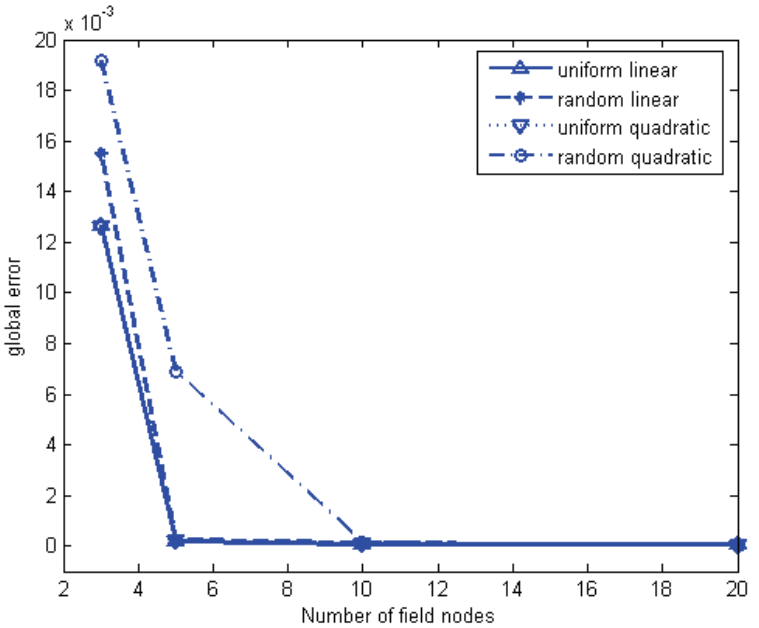

Figure 3: Variation of the global errors via the linear basis and quadratic basis with the number of field nodes distributed randomly and uniformly.

where

$$f(x) = -\frac{e^x(A\pi - eA\pi\cos(A\pi) + e\sin(A\pi))}{1+A^2\pi^2} + \sin(A\pi x) \tag{58}$$

with the exact solution $\varphi(x) = \sin(A\pi x)$, $A = 1, 2, \cdots 10$. [Babolian, Marzban and Salmani (2008)]. Here the kernel function is an exponential function and the exact solution is a periodic trigonometric function in this case. The problem is solved via 3, 5, 10, 20, 40 and 60 field nodes distributed randomly and uniformly respectively, with totally 90 virtual nodes following the cosine distribution pattern. The linear basis is employed hare as the polynomial basis. A is a natural number ranging from 1 to 10, and here it is taken as 4. Figs. 4 and 5 present the comparisons between the numerical results and the analytical solutions via the 60 field nodes distributed uniformly and randomly, respectively.

It is always found that the numerical solution coincides well with the analytical solution for the field nodes distributed randomly and uniformly. Fig. 6 illustrates the convergence rates for the two kinds of the distributions of the field nodes. It is observed that the numerical results converge to the analytical results as the nodal

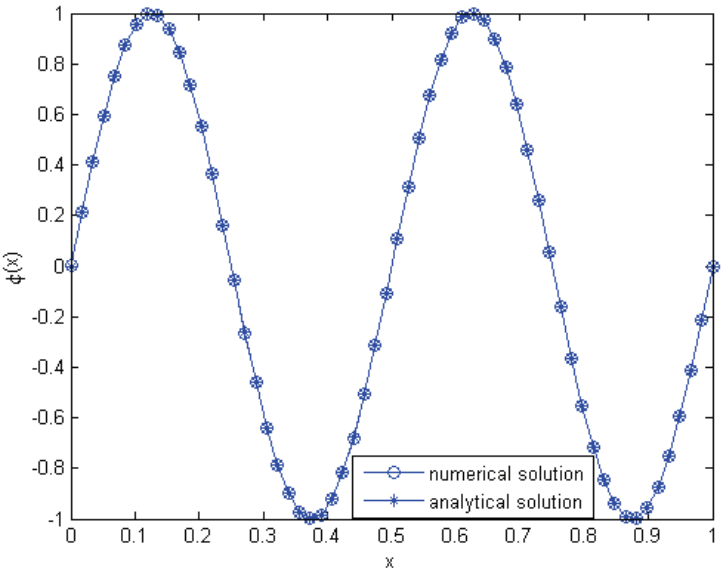

Figure 4: Comparison between the numerical and exact solutions for the second case study of 1-D Fredholm integral equation via the 60 field nodes distributed uniformly.

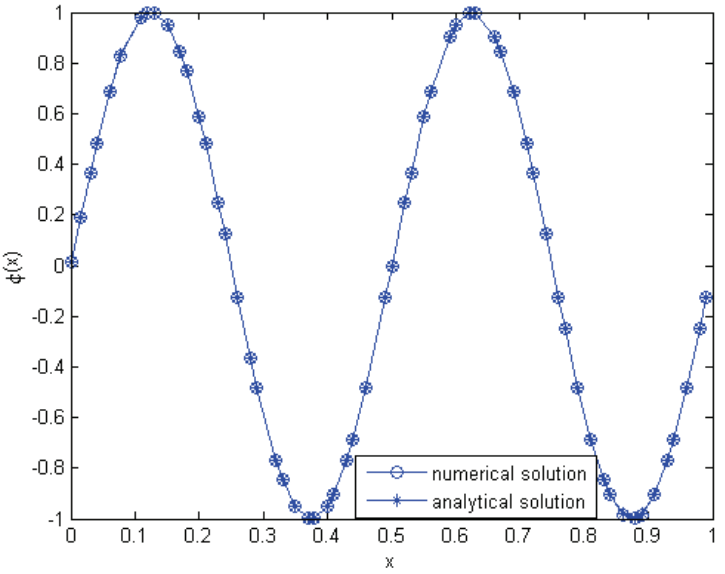

Figure 5: Comparison between the numerical and exact solutions for the second case study of 1-D Fredholm integral equation via the 60 field nodes distributed randomly.

spacing decreases. The convergence rate is equal to 3.2233 for the field nodes distributed uniformly, while the convergence rate is 2.6413 for the field nodes distributed randomly. Both of them converge fast.

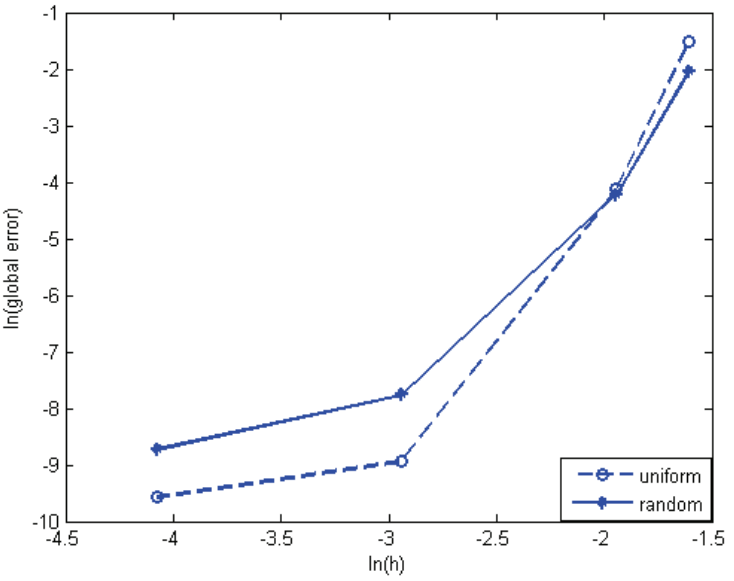

Figure 6: Convergence rates for the second case study of the 1-D Fredholm integral equation by field nodes distributed randomly and uniformly.

5.2 Two-dimensional Fredholm integral equation

The case study for the two-dimensional Fredholm integral equation is given as

$$\varphi(x,y) = \int_0^1 \int_0^1 xy\varphi(\xi,\eta)\,d\xi d\eta + \frac{3}{4}xy \tag{59}$$

with the exact solution $\varphi(x,y) = xy$. In order to solve this two-dimensional Fredholm integral equation, totally 400 virtual nodes with the 9, 36, 81, 144 and 225 field nodes scattered randomly and uniformly are used. The linear two-dimensional basis is used as the polynomial basis of the shape function. Figs. 7 and 8 demonstrate the comparisons between the numerical results and the analytical solution via the 100 field nodes distributed uniformly and randomly, respectively.

Fig. 9 is plotted to study the convergence rates for the field nodes distributed randomly and uniformly. It is observed from this figure that, as the number of field

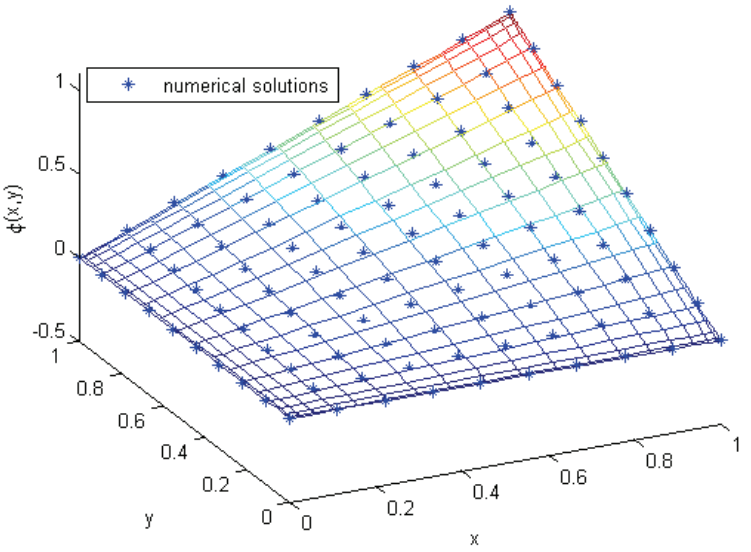

Figure 7: Comparison between the numerical and exact solutions for the case study of 2-D Fredholm integral equation via the 10×10 field nodes distributed uniformly.

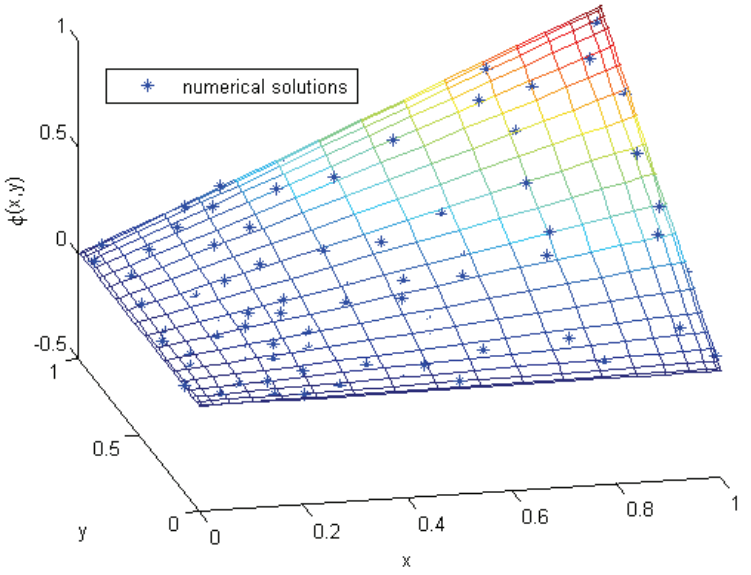

Figure 8: Comparison between the numerical and exact solutions for the cese study of the 2-D Fredholm integral equation via the 10×10 field nodes distributed randomly.

nodes increases, the global errors decrease for both the distributions of field nodes. The global error for the field nodes distributed randomly is larger than that for the field nodes distributed uniformly. However, the difference of the global errors becomes more and more ignorable as the number of field nodes increases. Actually the global errors are equal to 3.5443E-3 and 5.9444E-2 for the 9 field nodes, while they become 1.1966E-4 and 2.0752E-4 for the 225 field nodes respectively. The convergence rate is equal to 2.7684 for the field nodes distributed randomly, which is lager than 1.8428 for the field nodes distributed uniformly. It is thus concluded that the RIQ method can solve the two-dimensional Fredholm integral equations well via the field nodes distributed randomly or uniformly.

5.3 Three-dimensional Fredholm integral equation

It is easy to extend the two-dimensional Fredholm integral equation to the three-dimensional one. Here the case study is carried out to for the numerical solution of the three-dimensional Fredholm integral equation solved by the RIQ method.

Let's consider the following 3-D Fredholm integral equation

$$\varphi(x,y,z) = \int_0^1 \int_0^1 \int_0^1 xyz\varphi(\xi,\eta,\gamma)\,d\xi d\eta d\gamma + \frac{7}{8}xyz \tag{60}$$

with the exact solution $\varphi(x,y,z) = xyz$. The problem is solved via the $10\times10\times10$ fixed virtual nodes with the $3\times3\times3$, $6\times6\times6$, $9\times9\times9$ field nodes distributed randomly and uniformly. The global errors are obtained and listed in Tab. 1. It is seen that, with a few field nodes such as 27 field nodes, the global errors exactly 7.6079E-3 and 1.2466E-2, are small for the field nodes distributed randomly and uniformly. The global errors decrease as the number of field nodes increase. Fig. 10 shows how the numerical results converge to the analytical solution as the nodal spacing reduces. The convergence rates are equal to 2.1733 and 0.9051 for the field nodes distributed uniformly and randomly respectively.

Table 1: Global errors of the case study of the 3-D Fredholm integral equation by the field nodes distributed uniformly and randomly with $10\times10\times10$ fixed virtual nodes.

Field nodes	Virtual nodes	Error for the field nodes distributed randomly	Error for the field nodes distributed uniformly
$3\times3\times3$	$10\times10\times10$	7.6079E-3	1.2466E-2
$6\times6\times6$	$10\times10\times10$	3.2746E-3	1.4743E-3
$9\times9\times9$	$10\times10\times10$	2.1764E-3	6.3426E-4

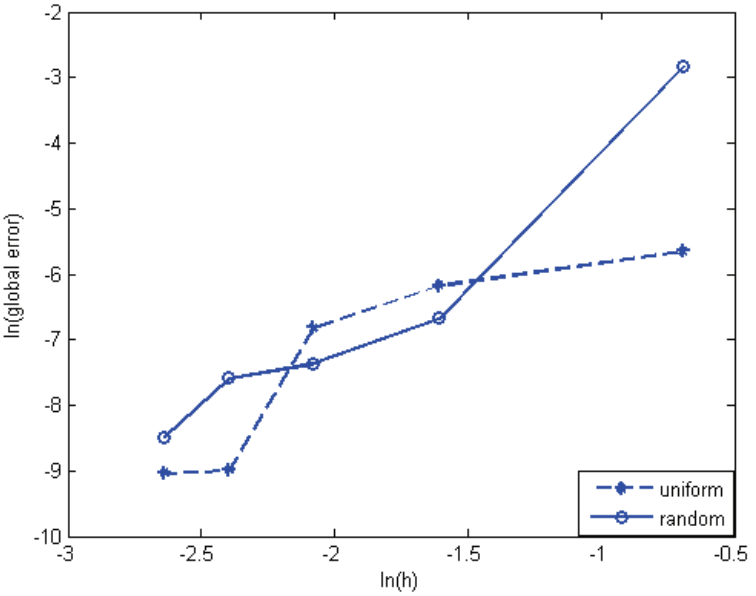

Figure 9: Convergence rates for the case study of the 2-D Fredholm integral equation by the field nodes distributed randomly and uniformly.

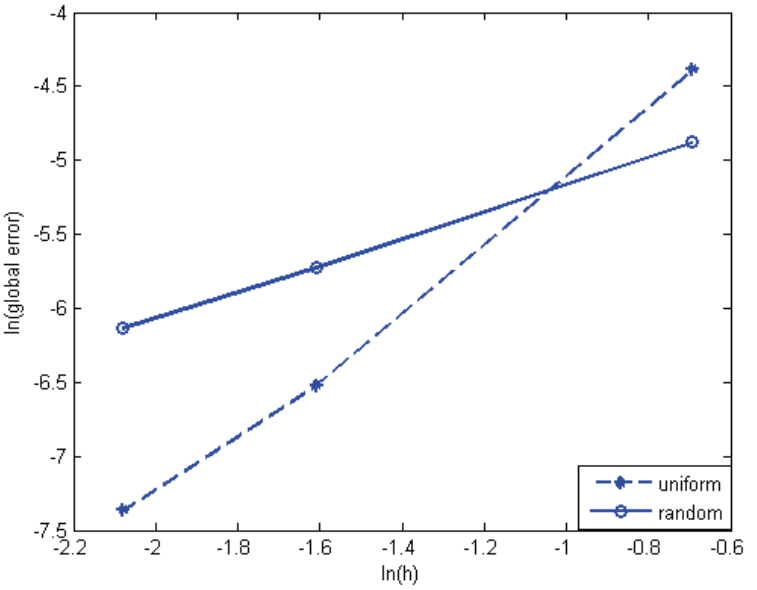

Figure 10: Convergence rates for the case study of the 3-D Fredholm integral equation by the field nodes distributed randomly and uniformly.

6 Conclusions

A novel meshless method has been developed in this paper and termed the random integral quadrature (RIQ) method, for solving the second kind of Fredholm integral equations in one-, two- and three-dimensional domains. In the RIQ method, the generalized integral quadrature (GIQ) technique is used first to discretize the integral governing equation over the virtual nodes. The Kriging interpolation technique is then employed to approximate the function values at the virtual nodes over all the field nodes. By this way, the RIQ method combines the GIQ technique with the Kriging interpolation approach together, and it can be used to solve the second kind of Fredholm integral equations via the field nodes distributed randomly or uniformly. After the detailed formulation of the RIQ method, several cases studies for the Fredholm integral equation in one-, two- and three-dimensional domains are conducted by the RIQ method. The numerical experiments reveal that the RIQ method can handle well this kind of integral equations in multi-dimensional domains, via the field nodes distributed randomly or uniformly. The convergence rate is also studied, and it is concluded that the numerical results always converge to the analytical solution fast.

Reference

Atluri, S. N., Zhu, T. (1998): A new Meshless Local Petrov-Galerkin (MLPG) approach in computational mechanics. *Computational Mechanics* 22, 117-127.

Babolian, E., Abbasbandy, S., Fattahzadeh, F. (2008): A numerical method for solving a class of functional and two dimensional integral equations. *Applied Mathematics and Computation* 198, 35-43.

Babolian, E., Marzban, H. R., Salmani, M. (2008): Using triangular orthogonal functions for solving Fredholm integral equations of the second kind. *Applied Mathematics and Computation* 201, 452-464.

Belytschko, T., Lu, Y. Y., Gu, L. (1994): Element-free Galerkin methods. *International Journal for Numerical Methods in Engineering* 37, 229-256.

Farnoosh, R., Ebrahimi, M. (2008): Monte Carlo method for solving Fredholm integral equations of the second kind. *Applied Mathematics and Computation* 195, 309-315.

Krige, D. G. (1951): A statistical approach to some basic mine valuation problems on the Witwatersrand. *Journal of Chemical Metallurgucal and Mining Societny of South Afirica* 52, 119-139.

Li, H., Ng, T. Y., Cheng, J. Q., Lam, K. Y. (2003): Hermite–Cloud: a novel true meshless method. *Computational Mechanics* 33, 30-41.

Li, H., Wang, Q. X., Lam, K. Y. (2004): Development of a novel meshless Local Kriging (LoKriging) method for structural dynamic analysis. *Computer Methods in Applied Mechanics and Engineering* 193, 2599-2619.

Liu, G. R., Zhang, J., Lam, K., Li, H., Xu, G., Zhong, Z., Han, X. (2008): A gradient smoothing method (GSM) with directional correction for solid mechanics problems. *Computational Mechanics* 41, 457-472.

Liu, W. K., Sukky, J., Yi Fei, Z. (1995): Reproducing kernel particle methods. *International Journal for Numerical Methods in Fluids* 20, 1081-1106.

Lucy, L. B. (1977): A numerical approach to the testing of the fission hypothesis. *The Astronomical Journal* 82, 1013-1024.

Maleknejad, K., Karami, M. (2005): Using the WPG method for solving integral equations of the second kind. *Applied Mathematics and Computation* 166, 123-130.

Mukherjee, Y. X., Mukherjee, S. (1997): On boundary conditions in the element-free Galerkin method. *Computational Mechanics* 19, 264-270.

Nayroles, B., Touzot, G., Villon, P. (1992): Generalizing the finite element method: diffuse approximation and diffuse elements. *Computational Mechanics* 10, 307-318.

Oñate, E., Idelsohn, S., Zienkiewicz, O. C., Taylor, R. L. (1996): A finite point method in computational mechanics and its applications to overcom transport and fluid flow. *International Journal for Numerical Methods in Engineering* 39, 3839-3866.

Rahman, M. (2007): *Integral equations and their applications*. WIT Press. Southampton.

Shu, C. (2000): *Differential Quadrature and Its Application in Engineering*. Springer. London.

Shu, C., Khoo, B. C., Chew, Y. T., Yeo, K. S. (1996): Numerical studies of unsteady boundary layer flows past an impulsively started circular cylinder by GDQ and GIQ approaches. *Computer Methods in Applied Mechanics and Engineering* 135, 229-241.

Shu, C., Khoo, B. C., Yeo, K. S. (1994): Numerical solutions of incompressible Navier-Stokes equations by generalized differential quadrature. *Finite Elements in Analysis and Design* 18, 83-97.